
# SEPARATION SAFETY ANALYSIS IN VARIABLE LAUNCH CONDITION OF SMALL AIR-LAUNCHED UAVS BASED ON NUMERICAL SIMULATION AND FLIGHT TEST

Guo Bin[1], Lu Yafei[1,*] , Wang Bo[2]， Guo Zheng[1], Jia Guowei[1] & Liu Duoneng[1]

[1]College of Aerospace Sciences and Engineering, National University of Defense Technology, Changsha, China, 410073

[2]National Innovation Institute of Defense Technology, Chinese Academy of Military Science, Beijing, China, 100171

## Abstract

Small air-launched UAVs are carried by the carrier aircraft, transported to the designated area, and launched on demand in the air, which have longer range, better maneuverability and flexibility. However, during the separation process, small air-launched UAVs are more susceptible to airflow disturbances, which could result in unstable flight attitudes and even collisions with the carrier. In order to evaluate the safety of the launch separation process of small folded UAVs launched from wing mounted tubes, numerical simulaiton and flight test method is present. XFlow software with lattice Boltzmann method is used for numerical simulation. Ignoring the influence of crosswind and carrier propeller, semi-simulation is used to obtain sub-aircraft flight trajectories in variable condition with different launch directions, carrier aircraft cruising speeds, launch speeds, and delayed unfolding time. Through the comparative of simulation results, a relatively ideal launch strategy is obtained: backward launch, cruising speed of 40m/s, launch speed of 5m/s, and delayed wing unfolding control. The experimental system is built and flight test was carried out. Results show that the carrier is basically unaffected under the recommended working conditions, the sub-aircraft drops 25m in height and 10m/s in speed within 20s after launch, the fluctuations of pitch angle, roll angle and heading angle do not exceed ±10°. the sub-aircraft can be deployed smoothly and safely detached from the carrier.

**Keywords:** Air-launched UAV; XFlow; launching safety analysis; Flight test

## Foreword

Small air-launched UAVs are widely used in modern battlefields, and gradually change the air combat mode[1][2]. These UAVs are carried by the carrier aircraft, transported to the designated area, and launched on demand in the air. They can cooperate with manned fighters to perform reconnaissance and suicide attack missions. Compared with the carrier aircraft, the electrically powered small air-launched UAV (i.e., sub-aircraft) is smaller in size, RCS, and noise, so it was difficult to be detected. Moreover, the sub-aircraft is flexible and low-cost, which means higher cost-effectiveness ratio to combat it[3][4].

The swarm UAVs can launch a saturation attack at a low cost, which also increases the enemy's defense cost[5], but the swarm drone is usually launched from ground or sea ships[6], and its range and duration are limited, usually less than one hour. Combined with the advantages of air-launched UAVs and swarm UAVs, each carrier aircraft could carry a number of sub-aircrafts, and after approaching the operational airspace, carrier aircraft launch sub-aircrafts outside the defense zone. The carrier aircraft can provide communication support for sub-aircrafts in the air. It can increase the range, flight time, maneuverability and flexibility of the sub-aircraft, and protect the carrier aircraft with higher value from the threat of attack.

Currently, the United States, Germany, Russia, and China are conducting research on air-launched UAVs[7][8]. The U.S. air-launched UAV projects include the "Gremlins"[9], "ALTIUS"[10], "Switchblade","Coyote"[11], "Sparrowhawk", "Unmanned Targeting Aerial System", and "Perdix" miniature air- launched UAV[12], among which the "Gremlins" UAV was successfully deployed from

the C130 transport aircraft in 2019 and achieved aerial recovery in 2021. The ALTIUS-600 UAV can be launched from the Black Hawk forward or from the Netan magazine of Valkyrie drone. Additionally, China's air-launched UAV research includes the FH-901 of CASC (China Aerospace Science and Technology Corporation), the LJ-1 UAV of Northwestern Polytechnical University, and the TS-10 low-speed UAV of Sichuan Tengden Sci-tech Innovation.

Although air-launched UAVs have many advantages, there are also many difficulties and risks in the launch process. In 1966, when an SR71 reconnaissance aircraft of the U.S. military dropped an MD21 drone in the air, the drone crashed back into the carrier aircraft, causing the SR-71 reconnaissance aircraft to disintegrate in the air. For UAVs launched from the carrier wing launch canister, when the sub-aircraft wings and vertical tails deploying, the aerodynamic characteristics are very varied[13]. While the sub-aircraft is small in size, and it is more sensitive to airflow disturbances, and has higher requirements for stability. During separation, accidents such as unfavorable wing deployment, unstable flight attitude, and even collision of sub-aircraft with the carrier may occur.Therefore, the conditions for launching sub-aircraft are strict, and it is necessary to simulate the launch trajectory of the sub-aircraft under different working conditions (such as different cruising speeds and different crosswind speeds) to explore the impact on the carrier aircraft, and obtain the safe delivery parameters under different launching conditions. These studies can provide a reference for the sub-aircraft to adjust the control strategy, and predict the risk of carrying out air-launched tests in an unsatisfactory wind field environment.

## 1. Numerical Simulation Methods

### 1.1 Physical model

The carrier aircraft used for simulation and flight test is the FX-0503 oil-activated long endurance fixed-wing UAV developed by our group, which carries two sets of spring-energy-storage launcher tube systems[14], including steel wire pulley sets, energy-storage springs, and adapted pistons[15], etc., under the wings on both sides of the carrier. The carrier adopts an aerodynamic layout with a large aspect ratio, a downward-reversing V-shaped tail, and a rear-mounted propeller, which provides high aerodynamic efficiency, longitudinal stability, and lateral stability, enabling it to maintain its own stability as much as possible when dropping off sub-aircrafts.

The sub-aircraft is powered by a battery, an electric motor and a two-bladed propeller, which produces low noise and low heat signatures[16]. It has a duck-type aerodynamic layout and is in a folded state before launching, with the front wings folded back, the rear wings and vertical tail folded forward. All airfoils are integrated with the fuselage, which is just placed in the launch tube. Upon receiving the launch command from ground control station, the rudder unlocks the launch tube's limiting device, and the energy storage spring provides the initial velocity for the sub-aircraft to launch.

The parameters of carrier and sub-aircraft are shown in Table 1 and the working process is shown in Figure 1. After the carrier aircraft dropind sub-aircrafts in sequence at an altitude of about 400 metres outside the defence zone, it rises to an altitude of 500 metres and hovers to provide communication safeguards for sub-aircrafts. These sub-aircrafts will approach, reconnaissance, strike the target and send back reconnaissance data to the carrier aircraft, and multiple sub-aircrafts can achieve coordinated operation.

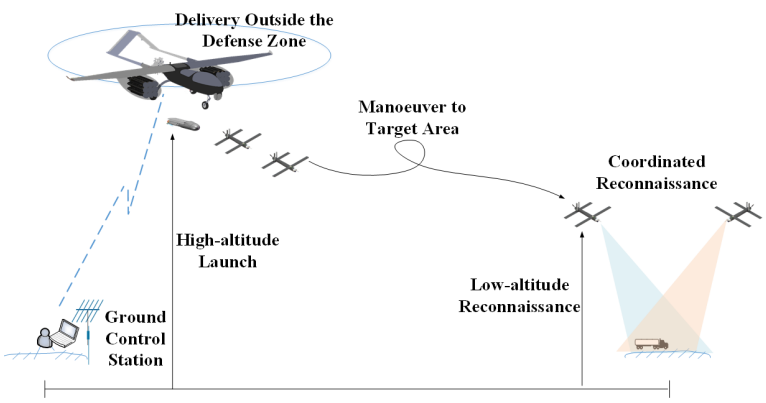


Figure 1 – Working process diagram of air-launched UAV.

Table 1 – Carrier and sub-aircraft characters.

| | Dimensions/m | $M$/kg | $x$/m | $I_{xx}$/(kg·m$^2$) | $I_{yy}$/(kg·m$^2$) | $I_{zz}$/(kg·m$^2$) |
|---|---|---|---|---|---|---|
| Carrier | 4.4×6.2×1.4 | 180 | 4.4 | 300 | 475.2 | 199.2 |
| Sub-aircraft | 1.3×1.6×0.3 | 8.9 | 1.27 | 0.9 | 0.9 | 0.8 |

In order to simplify the physical model, the launch tube system and the carrier propeller are omitted in simulation, and the initial launch velocity is simulated by directly setting the sub-aircraft velocity. Since both the carrier and the sub-aircraft are symmetrically laid out, no crosswind in the simulation process, and the two sides have little mutual coupling, the use of half-mode calculation does not affect the result analysis, and it can save computational resources and speed up the iteration. The carrier and sub-aircraft models are shown in Figure 2. In the ground coordinate system, the incoming flow direction is set as X-axis positive, the X-axis direction is consistent with the axial direction of carrier in level flight, and the plumb direction is set as Z-axis positive, and Y-axis direction is consistent with the lateral direction of carrier in level flight.

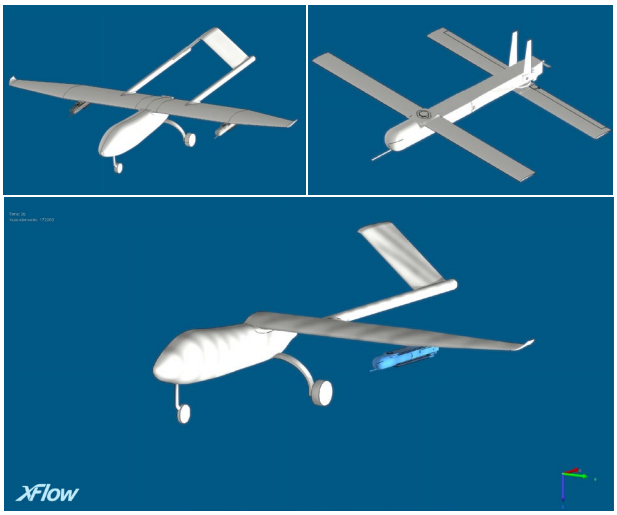


Figure 2 – Physical models of carrier and sub aircraft.

## 1.2 Simulation software

The simulation in this paper adopts Dassault's XFlow software, which uses the particle tracking method based on the Boltzmann model. The lattice Boltzmann method (LB) belongs to mesoscopic computational fluid dynamics, which is a highly efficient numerical tool in computational fluid dynamics (CFD), and compared with macroscopic and microscopic computational fluid dynamics, the lattice Boltzmann method based on the discretisation of the set of target macroscopic control equations, it greatly simplifies the equations in numerical simulation, and has clear physical meaning, simple boundary conditions, good parallelism, and easy implementation of the procedure.

XFlow software adopts large eddy simulation (LES) as the flow solver for complex turbulent flows[17]. The LES adopts the instantaneous NS equations to directly simulate the large-scale eddies in the turbulent flow, and the turbulent pulsation is modelled for the small-scale eddies (sub-lattice model), which can simulate the turbulent motion with higher Reynolds number and more complex turbulence, and efficiently solve the CFD problems involving the motion mechanism in the geometrical domain.

LES uses a filter function to decompose the flow variable $U(x,t)$ into a large-scale quantity $\overline{U}(x,t)$ and a small-scale quantity $u'(x,t)$. The large-scale quantity $\overline{U}(x,t)$ Substituted into the NS equations, the large-vortex simulation control equations satisfied by the large-scale quantity can be obtained.

$$U(x,t)=\overline{U}(x,t)+u'(x,t) \tag{1}$$

where $\overline{U}(x,t)$ is a large-scale quantity (low-pass pulsation) and $u'(x,t)$ is a small-scale quantity (residual pulsation)

$$\overline{U}(x,t)=\int G(r,x)U(x-r,t)\mathrm{d}r \tag{2}$$

where $G(r,x)$ is the filter function, and $\int G(r,x)\mathrm{d}r=1$

The filtered continuity equation:

$$\frac{\partial \overline{U}_i}{\partial x_i}=0 \tag{3}$$

The filtered momentum equation:

$$\frac{\partial \overline{U}_i}{\partial t}+\frac{\partial \overline{U}_i\overline{U}_j}{\partial x_j}=-\frac{1}{\rho}\frac{\partial \overline{p}}{\partial x_i}+\frac{\partial}{\partial x_j}\left(\nu\frac{\partial \overline{U}_i}{\partial x_j}\right)+\frac{\partial \tau_{ij}}{\partial x_j} \tag{4}$$

where $\tau_{ij}$ is the turbulent subgrid stress, and $\tau_{ij}=\overline{u_iu_j}-\overline{u}_i\overline{u}_j$

Based on particles and the complete Lagrangian functions, XFlow software enables meshless delineation of fluid regions. With automatic point pattern generation and adaptive optimisation, inputs can be minimised, thus the time and effort spent on meshing and pre-processing phases can be reduced. With XFlow's discretisation method, a small set of parameters can be used to easily control the base point matrix and can be adapted to complex surfaces and moving parts.

### 1.3 Simulation conditions

The simulation adopts three-dimensional, single-phase, isothermal model, and external flow field, using air as the fluid, and the launch height is around 400m, so the fluid parameters such as temperature, air pressure and density are set to be consistent with the sea level, as shown in Table 2. In this round of simulation, in order to study the influence of launch direction, cruise speed, launch speed and delayed unfloding on the launch trajectory, 7 control variables are set, as shown in Table 3.

Table 2 – Working conditions of simulation.

| Wind tunnel dimensions /m | Altitude /m | Temp /K | Densities /(kg·m$^{-3}$) | Dynamic viscosity /(Pa·s) | Simulation step /s |
|---|---|---|---|---|---|
| 100×40×60 | 400 | 288.2 | 1.225 | 1.789×10$^{-5}$ | 0.02 |

Table 3 – Control variables of simulation.

| Num | Cruise speed | Launch direction | Launch speed | Simulation time |
|---|---|---|---|---|
| 1 | 40m/s | Backward | 5m/s | 1s |
| 2 | 40m/s | Forward | 5m/s | 1s |
| 3 | 40m/s | Backward | 8m/s | 1s |
| 4 | 40m/s | Backward | 10m/s | 1s |
| 5 | 30m/s | Backward | 5m/s | 1s |
| 6 | 50m/s | Backward | 5m/s | 1s |
| 7 | 40m/s | Backward | 5m/s | 2s |

Since the sub-aircraft needs to unfold the wings and vertical tail when dropping, the sub-aircraft is divided into the fuselage and its 6 sub-components, including the front wings, rear wings and vertical tails on both sides, when importing the model separately. The motion of the carrier aircraft is set as rigid-body motion, and the motion of the sub-aircraft is set as rigid-body motion with superimposed forced rotation, and the unfolding motion is simulated by adopting the cubicinterpolation function and setting the forced rotation of the wings and vertical tail, the unfolding time of the wings from 0 to 90°

is set to be 1.05s~1.45s, and that of the vertical tail is set to be 1.25s~1.45s. A force of about 88N was applied to the subplane in the Z-axis direction, which is equivalent to a gravitational acceleration of 9.8m/s$^2$ .

The XFlow software can draw the mesh with simple settings, and the simulation uses the adaptive refinement and wake effect enhancement function. When the mesh is too dense, the iteration efficiency is too slow, as shown on the left side of Figure 3, the initial mesh number of a separate sub-aircraft is 0.89 million, while the simulation reaches 33 million in the 0.14s, and the simulation takes about 12 hours for 0.1s, and the further back the longer the time is; when the mesh is too sparse, the simulation is not precise enough, as shown on the right side of Figure 3, the starting mesh number is 0.12 million and the simulation reaches 2.58 million in the 0.74s. Therefore, in order to accurately and quickly simulate the placement process, the grid size is set so that each gap in the model contains at least two layers of grids. After the adjustment, the maximum solution scale of the calculation domain is set to 5 m. The solution scales for the carrier, sub-aircraft, and wake are set to 0.02 m, 0.01 m, and 0.04 m respectively, and the overall number of the starting grids is approximately 51.3 million.

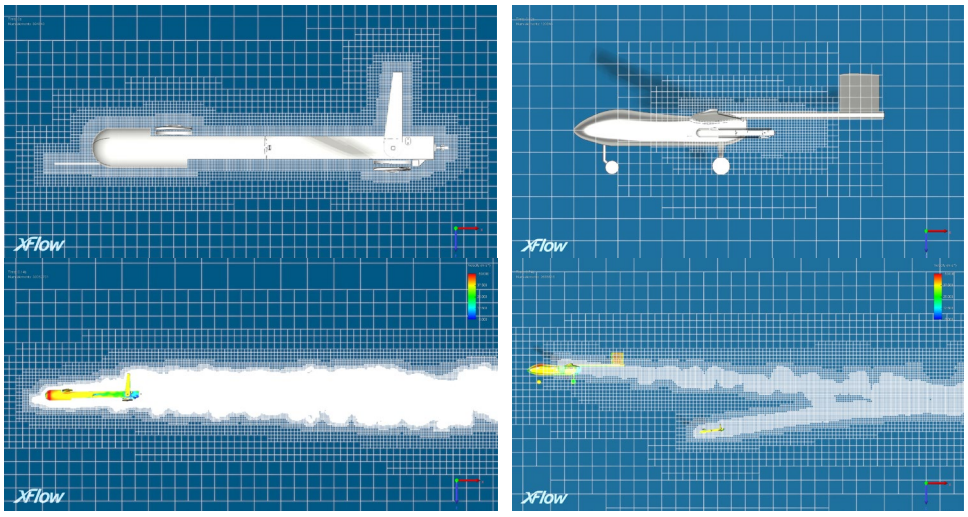


Figure 3 – Local computational scale and wake adaptive scale.

## 2. Simulation and Disscuss

### 2.1 Aerodynamic characteristics of sub-aircraft

Before the simulation of carrier airdropping sub-aircraft, the sub-aircraft aerodynamic characteristics in unfolding state are simulated, with the angle of attack of 0, the flight speed of 40m/s, and no crosswind. It can be seen from Figure 5 that the airflow passes through the sub-aircraft wing, fuselage, and vertical tail, and then a large number of vortices are formed at the tail end of sub-aircraft. Because there is no influence of the carrier, the tail trajectory of the sub-aircraft is basically horizontal, without up and down deviation.

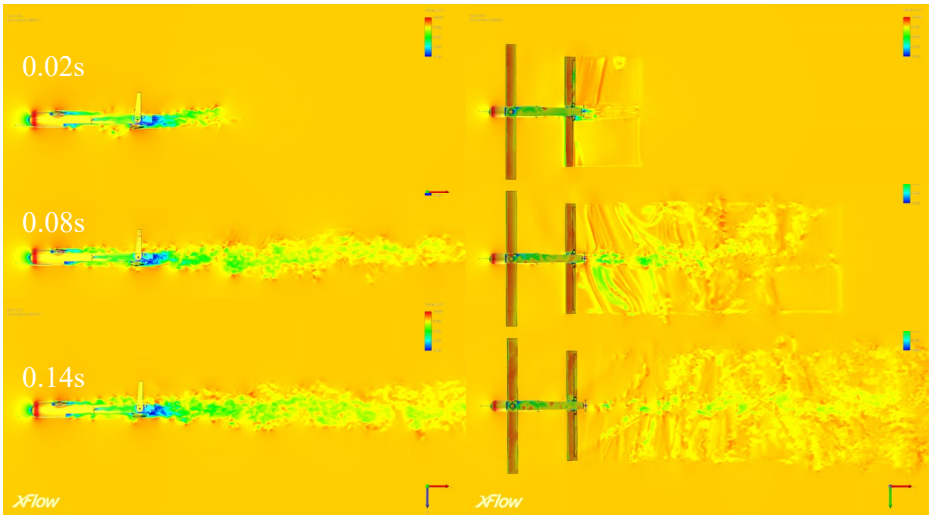


Figure 5 – Velocity cloud of the sub-aircraft in level flight.

Figure 6 shows the aerodynamic parameters of sub-aircraft in level flight, in which the lateral force coefficient Cy is basically stable at 0, fluctuating no more than ±0.05, which indicates that the lateral stability of sub-aircraft in level flight is very good, and it will not be offset left and right, and the drag coefficient Cx and the lift coefficient Cz fluctuates between 0 and 0.4 for the first 0.1s, and then stabilises above and below 0.2, which indicates that the sub-aircraft's aerodynamically efficient is high, and it is able to reduce the flight drag. Sub-aircraft can maintain the lift-weight balance and thrust-drag balance, and has good aerodynamic characteristics.

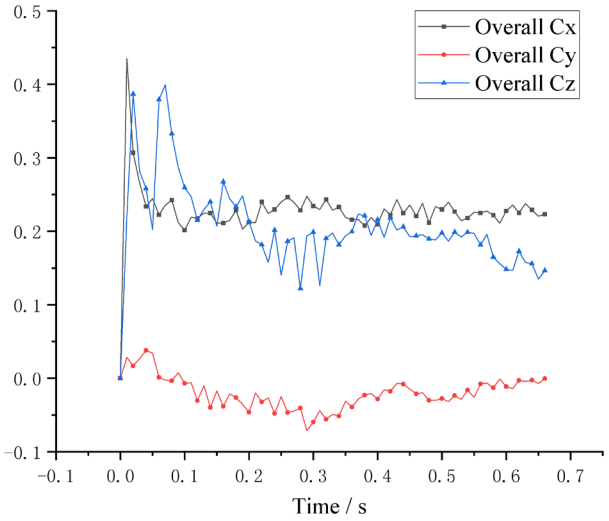


Figure 6 – Aerodynamic parameters of sub-aircraft in level flight.

## 2.2 Different launching directions

Under the working condition of cruise speed 40m/s, launch speed 5m/s, no crosswind, and no consideration of the influence of carrier propeller, the sub-aircraft with forward launch or backward launch can achieve safe separation. As shown in Figure 7, the sub-aircraft attitude have a slight head-down phenomenon, and there is basically no offset in the lateral direction, and as shown in Figure 8, the sub-aircraft are subjected to the Y-axis direction of the aerodynamic force can be ignored.

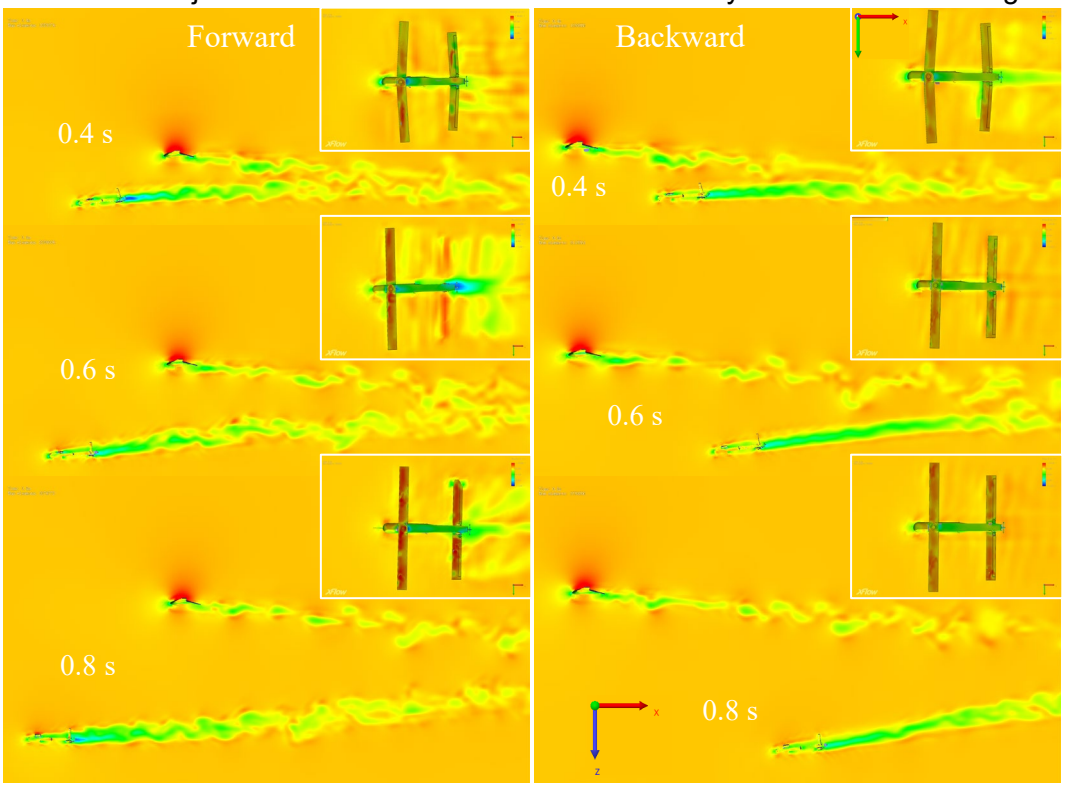


Figure 7 –Velocity cloud of sub-aircraft for forward and backward launch.

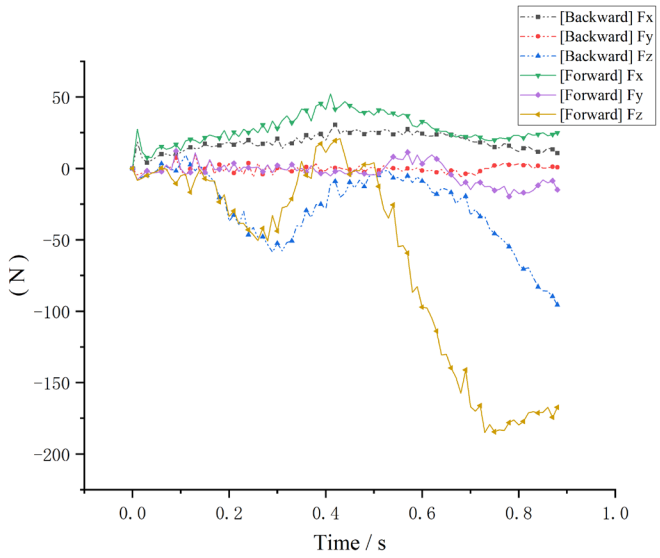


Figure 8 – Aerodynamic force of sub-aircraft for forward and backward launch.

While the tail track of sub-aircraft with forward launch has more overlapping area with that of carrier, and is more affected by the airflow of carrier. Secondly, the backward launch is more favourable for sub-aircraft to distance from carrier in the X-axis direction; and after sub-aircraft unfolding(0.5s~1s), the lift force of forward-launched sub-aircraft is almost twice as much as that of backward-launched one, and the tendency of forward-launched sub-aircraft to move upward is more obvious, and the risk of collision with carrier is also greater.

Therefore, although different launch directions can be safely separated under this condition, backward launch is more recommended, and the trajectory of the backward-launched sub-aircraft is shown in Figure 9.

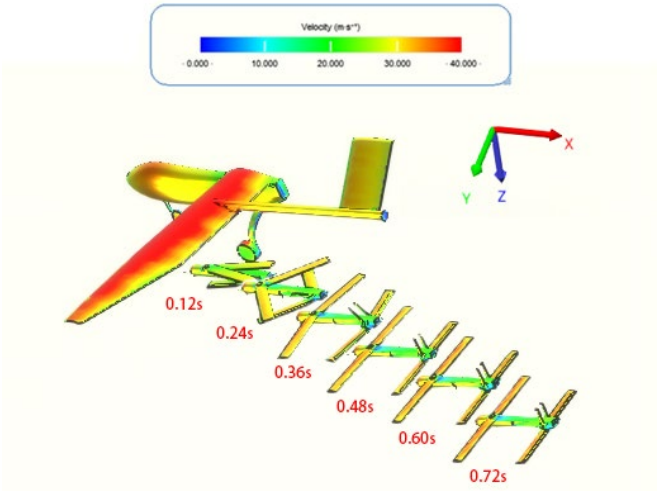


Figure 9 –Surface velocity cloud and sub-aircraft flight trajectories for forward launch.

## 2.3 Different cruising speeds

Under the working condition of backward launch, launching speed 5m/s, no crosswind, and no consideration of the influence of the carrier propeller, as shown in Figure 10 and Figure 11, the sub-aircraft can be smoothly deployed and safely launched under three kinds of cruising speeds of 30m/s, 40m/s, and 50m/s. The sub-aircrafts are subjected to basically the same transverse aerodynamic force, and the heading angles are all slightly shifted to the direction of the -Y-axis. When the cruising speed is faster, the vortex formed by the trails of carrier and sub-aircraft is more, so that sub-aircraft is more affected by the airflow. When the cruise speed is faster, the carrier aircraft is subjected to more lift, and the upward offset distance is larger, and the fluctuation range of the lift applied to sub-aircraft is larger between -80N and 70N, which makes it easier to be destabilised.

Therefore, a cruising speed of 40m/s or less is recommended, but when the cruising speed is too low, the sub-aircraft will also be slowed down after launching out of the tube, which is unfavourable to its

manoeuvrability and and lift effects, so cruising speed of 40 m/s is more appropriate.

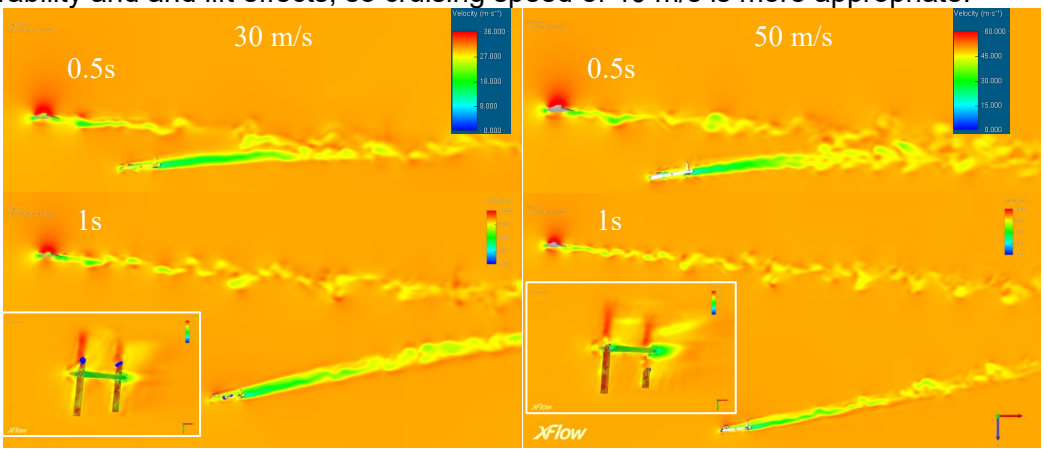


Figure 10 – Velocity cloud of sub-aircraft at different cruise speeds.

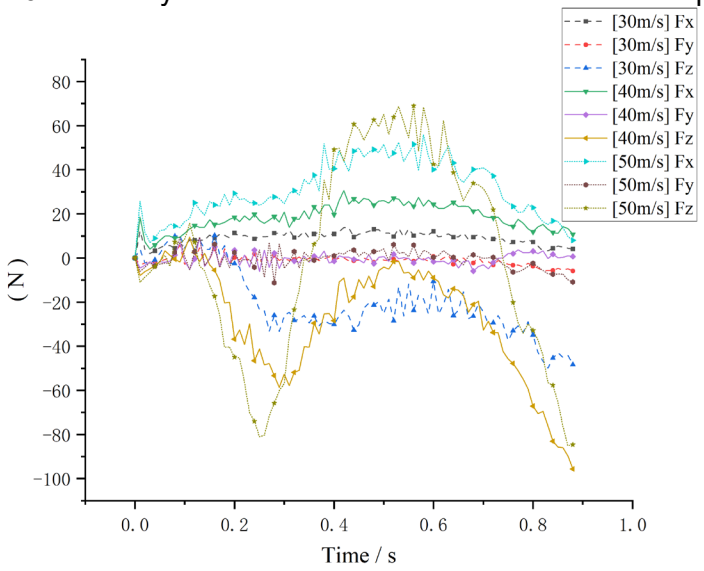


Figure 11 – Aerodynamic force of sub-aircraft at different cruise speeds.

## 2.4 Different launching speeds

Under the working condition of rearward launch, cruise speed of 40m/s, no crosswind, and no consideration of the influence of the carrier propeller, the simulation compares the trajectories of the sub-aircraft launching at different launching speeds (5m/s~10m/s). Figure 12 demonstrates the cutting velocity cloud of sub-aircraft with launch speeds of 8m/s and 10m/s, and it can be seen that the sub-aircrafts can safely separate at different launch speeds, and all of them can be detached from carrier's flow field region within 1s, and the flight attitudes are all smooth and very close to each other, with only a slight lateral offset to the inside of carrier.

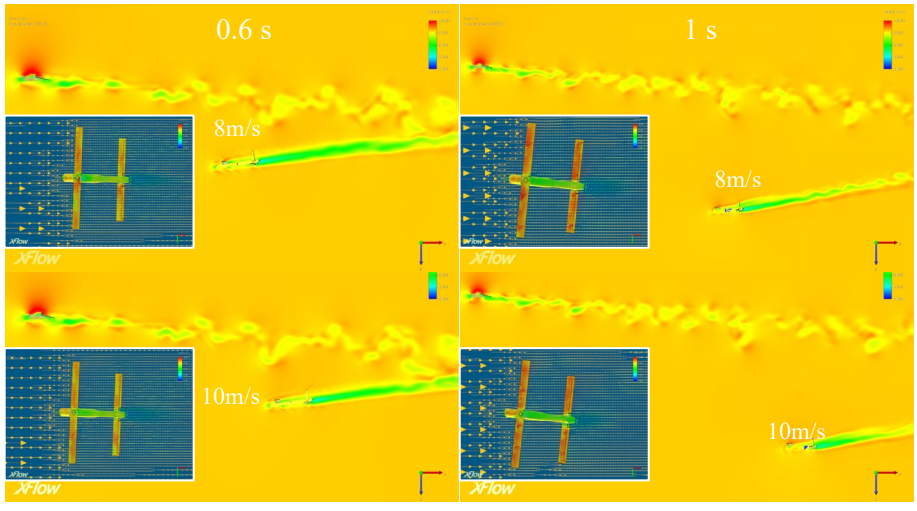


Figure 12 – Velocity clouds of sub-aircraft at different firing speeds（8m/s vs 10m/s).

As shown in Figure 13, the aerodynamic forces of sub-aircraft in all directions are basically the same for different launch speeds, fluctuating within the range of ±10N, so the launch speeds do not have much effect on the separation of the sub-aircraft. Although faster launch speed allows the sub-aircraft to separate from the carrier in the axial direction more quickly, the greater the launch speed, the greater the transient spring force that needs to be provided by the launch tube, and the more difficult it is to realise the faster exit speed in a launch tube of about 1m length.

Taking into account separation safety and the design of the launch tube, launch velocity of 5 m/s is recommended.

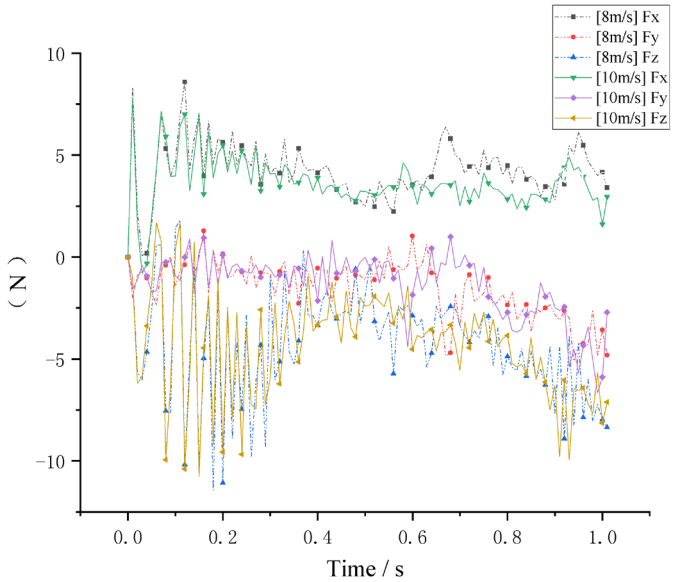


Figure 13 – Aerodynamic force of sub-aircraft at different firing speeds（8m/s vs 10m/s).

## 2.5 Sub-aircraft delayed unfolding after launch

Studies about air-delivered missiles and aerial bombs are more than air-launched UAVs and the technology is relatively mature[18]. Compared with air-delivered aerial bombs, the biggest difference between air-launched folding UAVs is that the sub-aircraft needs to unfold after launching, and the risk is also mainly focused on that process. If the delayed unfolding of the wings after sub-aircraft comes out of the launch tube, its launching process is similar to the air-dropped aerial bomb, and it is predicted that the interference of sub-aircraft in the folding state by the airflow of the carrier will be greatly reduced. Based on this idea, the sub-aircraft is set to unfold the wings at 1.05s~1.45s after launch and the vertical tail at 1.25s~1.45s.

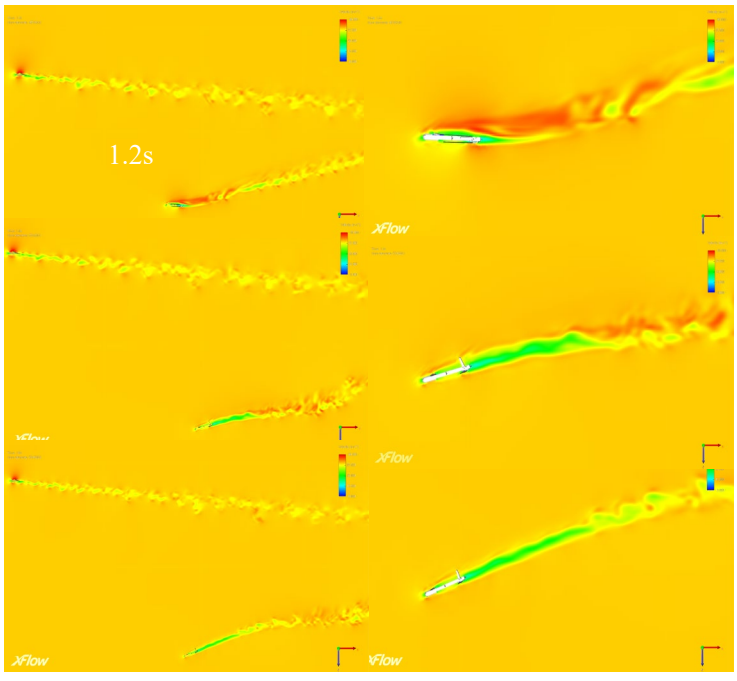


Figure 14 – Velocity cloud of sub-aircraft unfolding with a 1s delay after launchting.

As shown in Figures 14 and 15, the sub-aircraft is already out of the carrier wake region when the wings are deployed, and in the process the sub-aircraft is subjected to a large upward aerodynamic force, which reaches a peak value of 150N at 1.25s, causing the attitude of the airframe to shift from a slight head-up to a downward flight, and the pitch angle changes from about +2° to -30°. In the lateral direction, the aerodynamic force on the sub-aircraft is negligible, and there is almost no deflection of the sub-aircraft in the lateral direction as seen in the simulation trajectory.

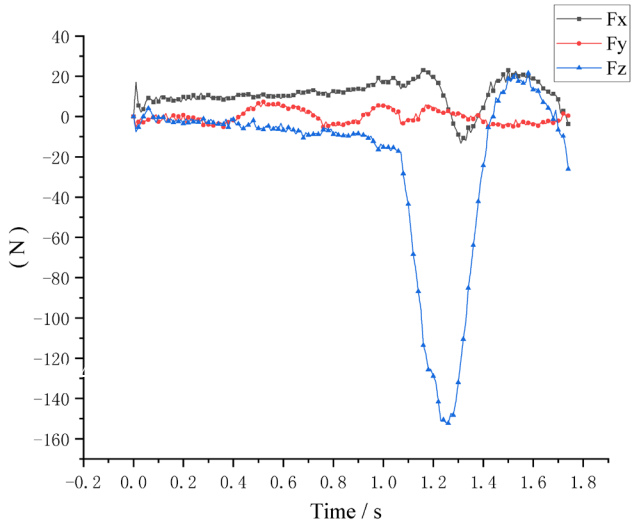


Figure 15 – Aerodynamic force of sub-aircraft unfolding with a 1s delay after launchting.

Therefore, when launching the sub-aircraft, if sub-aircraft is delayed for 1s to unfold, it can deviate from the carrier faster and avoid the risk of sub-aircraft crashing back to the carrier. However, because the unfolding of sub-aircraft is set to forced rotation during the simulation process, and the control ability of the subaircraft may not be able to pull it back to the level flight state when in actually air drop, and the subaircraft may have the risk of unfolding failure due to the influence of aerodynamic force.

## 3. Flight test and data analysis

During the flight test, the carrier aircraft carried two sub-aircrafts under wings, with a cruising speed of 40 m/s and a backward launch speed of 5 m/s, and maintained a attack angle of about 2° during the launch. The carrier launched one sub-aircraft for 8s before launching another sub-aircraft, reserving time to adjust the attitude of the carrier and reserving a safe distance for two sub-aircrafts. Taking the launching and separating process of one sub-aircraft for example, the actual separation process photographed on site is shown in Figure 16, and it can be found that the unfolding process and flight attitude of sub-aircraft are consistent with the simulation result Figure 9, and the sub-aircraft could smoothly unfold after launching, and carrier's attitude basically remained unchanged. However, in the first two pictures in Figure 16, the sub-aircraft was close to the carrier, and under the influence of carrier airflow, the sub-aircraft underwent a mild rolling movement, with a tendency to deflect to the inside of the carrier. Then sub-aircraft distanced itself from the carrier and was able to achieve a safe separation with a stable flight attitude.

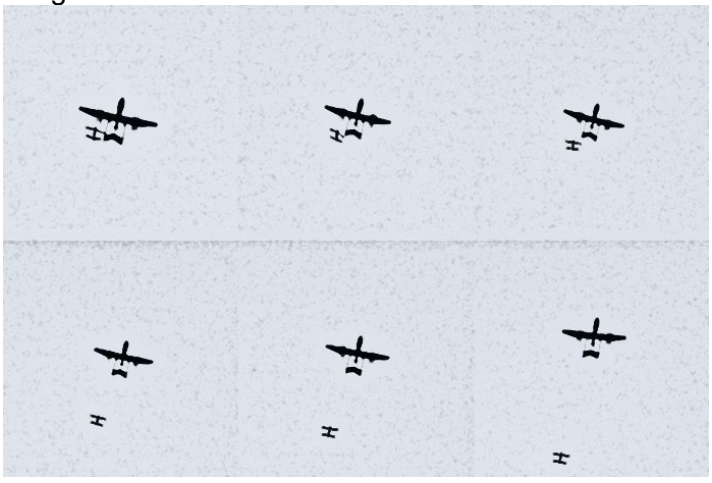

Figure 16 – Separation process of right side sub-aircraft.

Flight trajectories of carrier and sub-aircraft, before and after launching, were shown in Figure 17. It can be seen that sub-aircraft came out of the tube at the 66th second, and after launching, sub-aircraft avoided being interfered by carrier by quickly adjusting its attitude to get out of the carrier's course. The altitude curves and velocity curves of sub-aircraft and carrier are shown in Figure 18. Before and after the separation of sub-aircraft, the velocity of carrier fluctuated slightly, but basically there was no change, and it was maintained at about 40m/s. The velocity of sub-aircraft started to fluctuate with that of the carrier. The sub-aircraft speed at the beginning was the same as that of carrier, and within 20 seconds of launching the tube, sub-aircraft dropped 25m in height, after which its height was maintained at about 380m; the speed of sub-aircraft's velocity dropped from 40m/s to 30m/s, after which its speed was maintained at about 30m/s.

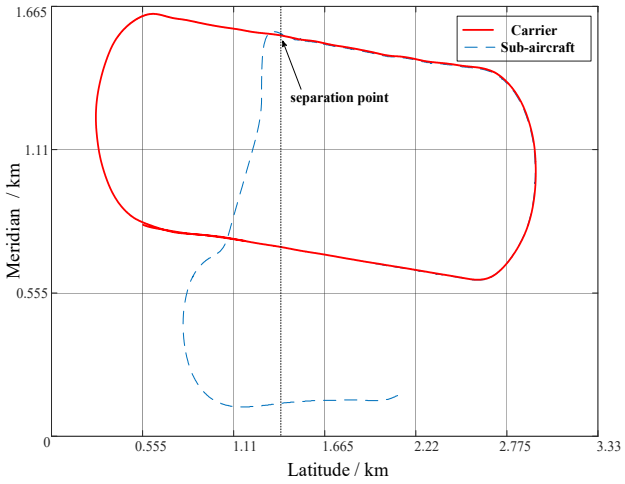


Figure 17 – Track diagram of sub-aircraft and carrier aircraft.

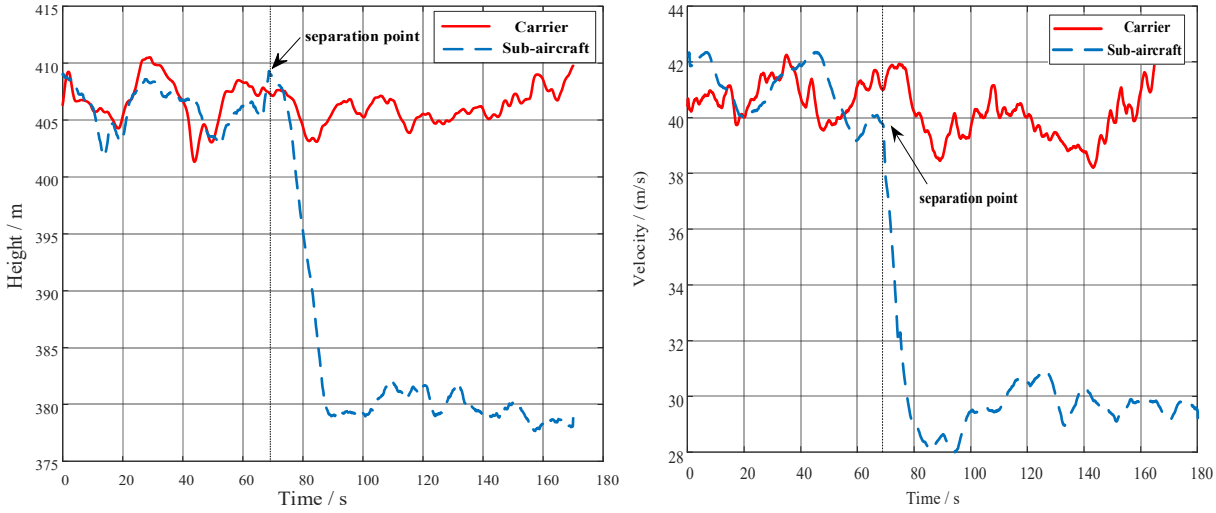


Figure 18 – Height change curve (left) and speed change curveand (right).

Figure 19 shows the sub-aircraft's attitude curves of pitch angle, roll angle, heading angle and the throttle response, as well as the carrier's pitch angle curves. The sub-aircraft launched at about 66s, and its paddles started working at about 68s. It can be found that the pitch angle of carrier only fluctuated slightly within ±2° in the 10s before and after launching, and there was almost no change, which once again verified that the carrier's flight attitude is not affected by the separation of sub-aircraft. While the sub-aircraft was affected by the carrier airflow, its pitch angle changed from 0 to 8° within 2s after launching, and with the start of sub-aircraft paddles, its pitch angle decreased to 0 and stabilises. If sub-aircraft's velocity is too fast after exiting the launch tube, it has a tendency to raise its head in 2s after launching, and there exists a possibility of crashing into the carrier, so adopting backward launching and delayed start of sub-aircraft paddles is conducive to the deceleration of subaircraft, which improves the separation safety. Between the 7th second and 19th second after launching, the sub-aircraft's heading angle and roll angle changed drastically: the roll angle changed from -3° to 30° and then decreased to 0, and the heading angle changed from -4° to 84°, which indicated that the subaircraft started to cut into the control and deviated from the carrier's course voluntarily after a period of time of throttle activation, which corresponded to the sub-aircraft deviating

from carrier's course by about 90° in Figure 17.

Overall, the sub-aircraft is able to achieve a safe separation under the recommended working conditions.

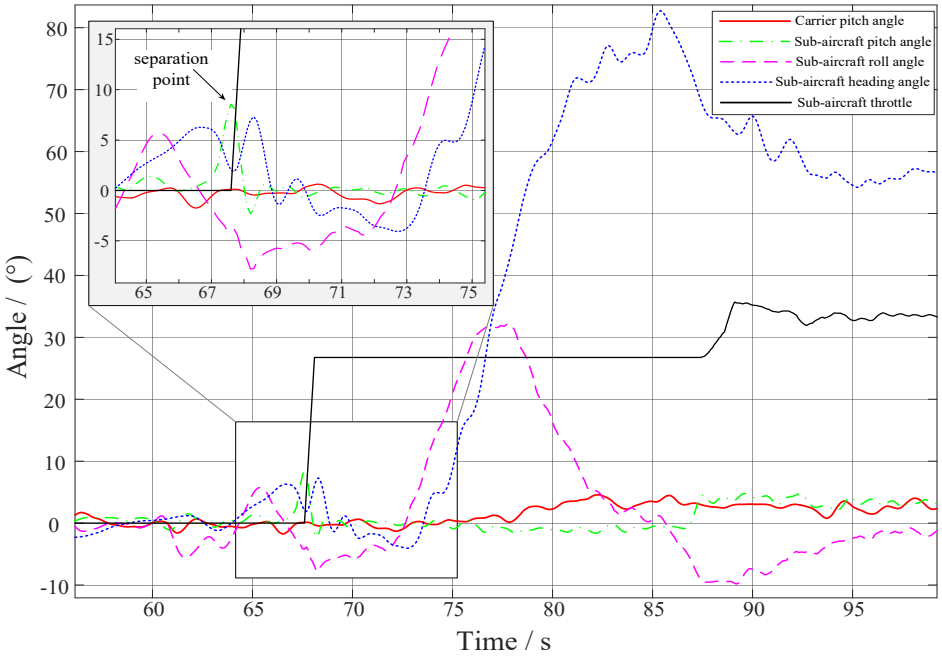


Figure 19 – Flight attitude change curve of sub-aircraft and carrier aircraft.

## 4. Conclusions

For the small folding UAVs launched from the carrier's wing-mounted launch tube, the model is simplified without considering the effects of crosswind and the carrier's propeller, and the launch trajectories of sub-aircraft for different launch directions, cruise speeds, launch speeds, and different unfolding times are simulated by XFlow software. Combined with the simulation results, flight tests are carried out and the following conclusions are obtained.

(1) Semi-simulation results show that under non-extreme working conditions, the safe separation of the sub-aircraft can be achieved regardless of forward or backward launch, the cruising speed of the carrier between 30m/s~50m/s, and the launching speed of the sub-aircraft between 5m/s~10m/s. However, the distance and the overlapping area of the tail track between sub-aircraft and carrier at the same time may be different under different working conditions. The recommended launch conditions are backward launch, cruise speed 40m/s, and launch speed 5m/s.

(2) Under the above recommended working conditions, the actual flight test data show that carrier aircraft has a smooth flight attitude throughout the whole flight, basically unaffected by the separation of sub-aircraft, and the sub-aircraft drops 25m in height and 10m/s in speed within 20s after launch, the fluctuation of the pitch angle, the roll angle, and the heading angle is not more than ±10°, and the sub-aircraft is able to smoothly unfold and safely detach itself from the carrier aircraft.

(3) The process of sub-aircraft unfolding delayed 1s after launch is simulated, and the results show that the sub-aircraft has already detached from the carrier wake region when unfolding the wings, and theaerodynamic force of sub-aircraft in the transverse direction is subjected to negligible, with almost no deflection, but the pitch angle is changed from about +2° to -30°, and detaches from carrier in that attitude. From the simulation, the delayed unfolding of the sub-aircraft after launch has the possibility of safe separation, but it requires that sub-aircraft has the control capability to pull it back from a pitch angle of -30° to a level flight state.

## 5. Funding

The research is sponsored by the Major Projects of Science and Technology Innovation 2030 (2021ZD0140300).

## 6. Contact Author Email Address

contact author email: 877411443@qq.com

## 7. Copyright Statement



## References

[1] YIN J, TAN L, TAN S J. Combat Application and Development Trend of Unmanned Aerial Vehicles (UAVs) in the U.S. Army[J]. *Aeronautical Missile*, 2010, (8): 26-29+33.

[2] WU H, DONG K, XU J. The future development trend of UAV and anti-UAV from the perspective of Russia-Ukraine conflict[J]. *Tactical missile technology*.

[3] Javier Jordan. The future of unmanned combat aerial vehicles: An analysis using the Three Horizons framework[J]. *Futures*, 2021, Vol.134: 102848.

[4] Stephen M. Biship, Kevin Curtis, Bolanle Sobande. Air-Launched Expendable Small Unmanned Aircraft Systems: Increasing Power and Extending Endurance to Meet Operational Needs[A]. *SAE Power Systems Conference*[C], 2010.

[5] Manel Khelifi, Ismail Butun. Swarm Unmanned Aerial Vehicles (SUAVs): A Comprehensive Analysis of Localization, Recent Aspects, and Future Trends[J]. *Journal of Sensors*, 2022, Vol.2022.

[6] WANG L Z, ZHAO X J, ZHANG Y. Unmanned aerial vehicle swarm mission reliability modeling and evaluation method oriented to systematic and networked mission[J]. *Chinese Journal of Aeronautics*, 2021, Vol.34(2): 466-478.

[7] US Air Force. *Unmanned Aircraft Systems Flight Plan 2009-2047*, 2009.

[8] US Department of Defense. *Unmanned systems integrated roadmap FY 2011-2036*, 2011.

[9] Rachel S. Karas.Air Force, DARPA sign Gremlins MOU as service plans future of small UAV[J]. *Inside the Air Force*, 2016, Vol.27(43): 6-7.

[10] LU Y F, HOU Z X, GUO Z. The development and technical difficulties of the ALTIUS small air-launched Unmanned Aerial Vehicle [J]. *National Defense Science and Technology*, 2022, 43(2): 27-32.

[11] DUAN H B, YANG Q, DENG Y M. Unmanned aerial systems coordinate target allocation based on wolf behaviors[J].Science China(Information Sciences), 2019, Vol.62(1): 205-207.

[12] Gareth Jennings. US demonstrates 'one of the world's largest' micro-UAV swarms[J]. *Jane's defence weekly*: IHS Jane's defence weekly, 2017, Vol.54(3): 12.

[13] DU X Q, MA G C, LI F. Aerodynamic Interference of Unmanned Aerial Vehicle (UAV) Missile Launch on Wings[J]. *Journal of Projectiles*, Missiles and Guidance, 2015, (3): 130-133.

[14] HOU Z X, LU Y F, WANG P. Air-launched UAV launch canister[P]. Chinese Patent: CN113120251A, 2021.07.16.

[15] GUO Z, LU Y F, WANG Y J. Air-launched unmanned aerial vehicle (UAV) launch system[P]. China Patent:CN113335502A, 2021.09.03.

[16] LU Y F, CHEN Q Y, WANG P. et al. Design and experiment of a small air-launched UAV[J]. Acta Aeronautica et Astronautica Sinica, 2023, 44(15): 528642.

[17] HE Y L, WANG Y, LI Q. *Theory and application of lattice Boltzmann method*[M]. Beijing:Science Press, 2009.

[18] GAO Q, CHANG H J, SUN X Q. Analysis and Experimental Study of Airborne Weapon Ejection and Delivery System Gas-Rigid-Flex Coupling[J]. *Intensity and Environment*, 2021, Vol. 48(4): 1-6.